PAPER

Large Code Set for Double User Capacity and Low PAPR Level in Multicarrier Systems

Khoirul ANWAR[†a)], ***Student Member***, **Masato SAITO**[†], **Takao HARA**[†], ***and*** **Minoru OKADA**[†], ***Members***

SUMMARY In this paper, a new large spreading code set with a uniform low cross-correlation is proposed. The proposed code set is capable of (1) increasing the number of assigned user (capacity) in a multicarrier code division multiple access (MC-CDMA) system and (2) reducing the peak-to-average power ratio (PAPR) of an orthogonal frequency division multiplexing (OFDM) system. In this paper, we derive a new code set and present an example to demonstrate performance improvements of OFDM and MC-CDMA systems. Our proposed code set with code length of N has $K = 2N + 1$ number of codes for supporting up to $(2N + 1)$ users and exhibits lower cross correlation properties compared to the existing spreading code sets. Our results with subcarrier $N = 16$ confirm that the proposed code set outperforms the current pseudo-orthogonal carrier interferometry (POCI) code set with gain of 5 dB at bit-error-rate (BER) level of 10^{-4} in the additive white Gaussian noise (AWGN) channel and gain of more than 3.6 dB in a multipath fading channel.

key words: *spreading code, OFDM, MC-CDMA, peak-to-average power ratio (PAPR), pseudo-orthogonal code, Carrier Interferometry (CI)*

1. Introduction

Multicarrier systems which decomposes a single wideband channel into a set of orthogonal narrowband channels is suitable for a high speed applications on the multipath fading environment. Within this family, the most commonly used scheme is the orthogonal frequency division multiplexing (OFDM), which is based on a discrete Fourier transform (DFT), resulting in an implementable technology and high performance structure with the fast Fourier transform (FFT). The OFDM is also widely believed to be a technology that has a bright future in many next generations of wireless communications systems [1]. This is because the multicarrier systems make fading over subcarrier become a frequency-non-selective (the bandwidth of each subcarrier is narrow enough in comparison to the coherent bandwidth of the fading channel). In addition, the insertion of a guard interval (GI) mitigates the inter-symbol interference (ISI) which is caused by the delay spread.

A combination of an OFDM and a code division multiple access (CDMA), called as multicarrier code division multiple access (MC-CDMA) has also been drawing much attention as an alternative to the conventional direct-sequence CDMA (DS-CDMA) system [2]. Each user's data are transmitted over the same set of subcarriers but with a unique spreading code to guarantee their separability (because of its orthogonality) at the receiver. If the number of and spacing between subcarriers are appropriately chosen in order that all subcarriers do not undergo a deep fading, the transmitted data can be reconstructed from the subcarrier which has no deep fading. It is the reason why full frequency diversity can be achieved by assigning a (frequency domain) spreading code prior to the inverse fast Fourier transform (IFFT) in OFDM and MC-CDMA systems. This assignment provides better bit-error-rate (BER) performances due to the frequency diversity benefits.

In the conventional OFDM with a spreading code [3] and MC-CDMA [4] systems, each user's data bit is transmitted simultaneously over N narrowband subcarriers where each subcarrier is encoded with an orthogonal combination of $+1$ or -1 (Walsh-Hadamard code). However, the Walsh-Hadamard code is not an optimum spreading code in terms of diversity benefit, because of the appearance of bad pairs of vectors (due to the limited number of distinct elements) that reduce the diversity gain as shown in [5]. In [6], Carrier Interferometry (CI) code, a complex spreading code, was introduced and its low computational complexity design have been presented in [7]–[9]. CI code has better peak-to-average power ratio (PAPR) performances than the Hadamard code in the OFDM system as shown in [10].

Recently, an interest to increase the capacity of multicarrier system such as OFDM and MC-CDMA systems is attracting many studies to develop a new spreading code for a larger data or user capacity. The number of codes, called as 'code-number,' can be increased from N to $K = N + A$, where $A \leq N$, while the length of the code, called as 'code-length,' is kept to N. The purpose is to acquire a higher user capacity, such as two orthogonal code set (TOCS) [11], quadriphase code [12], pseudo-orthogonal gold code (POGC) [13] and pseudo-orthogonal carrier interferometry (POCI) code [13]–[15]. Among these codes, POCI is the most attractive one in a better BER performance and its capability to reduce the PAPR level of the OFDM signals. In addition, the POCI's Implementation is becoming uncomplicated via double FFTs (with N additional constant separators of $\{e^{j(\frac{\pi}{N} \cdot n)}\}$ on each subcarrier for the second data set) as presented in [8].

As shown in [16] and later in [17], the cross-correlation amongst codes in the POCI code set is not low enough to mitigate the BER performance degradation (especially for multilevel modulations). High cross-correlations cause in-

Manuscript received July 9, 2007.
Manuscript revised March 7, 2008.

[†]The authors are with the Graduate School of Information Science, Nara Institute of Science and Technology, Ikoma-shi, 630-0192 Japan.
a) E-mail: anwar-k@is.naist.jp

DOI: 10.1093/ietfec/e91–a.8.2183

tercode interferences in the code set. The POCI code has a problem of large cross-correlations (both real and imaginary parts) which lead to the performance degradation. In addition, the cross-correlations of the POCI code are nonuniform between the code sets.

The nonuniform cross-correlation causes the signals to have un-equality in the probability of errors [18] amongst the assigned users. Therefore, a code set with lower and uniform cross-correlations is required to guarantee a fairness in multiuser systems. If the cross-correlations are uniform, the signal has an equal 'a priori probability' that result in a minimum error. Literatures [18] and [19] were pointed out that the desirable code set has uniform and low cross-correlation property. Although one could construct a code set having a uniform cross-correlation property, the code set size will diminish. It was also pointed out though one could construct a set of code in which all cross-correlations were equal (uniform), it comes to diminish in the size [18]. Consequently, finding the optimum large code set in terms of minimal cross-correlation is very difficult in general [20].

With some difficulties and limitations of constructing good code sets, in this paper, we try to improve the performance of OFDM and MC-CDMA systems by proposing a new large code set called large carrier interferometry (LCI) code. The proposed LCI code set has length of N but is capable of supporting $(2N + 1)$ data symbols or maximum $(2N + 1)$ users. We derive a new code set that satisfy uniform low cross-correlations to guarantee minimal BER performance degradation and at the same time reduce the PAPR level of the OFDM system. In addition, there is no restriction in the LCI code size. Therefore, any values of N are acceptable in the proposed LCI code.

To present a fair performance evaluation, we consider a comparison with the POCI code to show the effectiveness of the proposed LCI code. The POCI outperforms other pseudo-orthogonal codes as in [13], [14] and [15], therefore a comparison with other large code sets is enough by comparing the proposed LCI code with the POCI code. An example is presented for a length of $N = 16$. Our results confirm that the proposed LCI code offers a BER improvement more than 6 dB in the additive white Gaussian noise (AWGN) channel and more than 4 dB in a multipath fading channel compared with that of the POCI code.

The remainder of this paper is as follows. Section 2 describes the considered system model of OFDM and MC-CDMA systems. The derivation of the proposed LCI code is presented in Sect. 3 followed by its cross-correlation properties analysis in Sect. 4. Performance evaluation of the PAPR is presented in Sect. 5, while Sect. 6 provides BER performance evaluations for both OFDM and MC-CDMA systems. Section 7 concludes the paper.

2. System Model

Figure 1(a) shows the transmitter structure of the OFDM with a spreading code and Fig. 1(b) shows that of the MC-CDMA system. The incoming data symbols are converted from serial to parallel data stream. In the current OFDM system, each data symbol is modulated onto its own subcarrier and sent over the channels. Here, in the OFDM with a spreading code, each data symbol is multiplied by a spreading code $C(k, n)$, then spread-out onto all subcarriers, where k is data index of the OFDM (or user index in the MC-CDMA system) and n is the subcarrier index.

As shown in Fig. 1(a), one subcarrier holds N different data symbols. To separate the k-th data symbol, ($d(k)$, from the other $(N-1)$ data symbols in N subcarriers, the spreading code $C(k, n)$ with low cross-correlation properties should be selected. In the current OFDM and MC-CDMA systems, the $C(k, n)$ is Hadamard spreading code with a size of $N \times N$ and noted as $C(k, n)_{(N\times N)}$. However, to increase the user capacity or assign additional data symbols, the size of the spreading code should be $K \times N$, where $K > N$ and noted as $C(k, n)_{(K\times N)}$. Further, these $C(k, n)_{(K\times N)}$ is called as a large spreading code in this paper.

We substitute $C(k, n)_{(N\times N)}$ with the larger code $C(k, n)_{(K\times N)}$ i.e. the POCI code and the proposed LCI code to achieve a higher capacity of $K > N$. Further, $C(k, n)_{(K\times N)}$ is noted as $C(k, n)$ for a simple expression. Using $C(k, n)$, we spread the input data symbols to obtain a spread data $D(i)$ and generally expressed as

$$D(i) = \frac{1}{\sqrt{K}} \sum_{k=0}^{K-1} d(k) \cdot C(k, i), \tag{1}$$

where $d(k)$ is the k-th data symbol and $i = 0, 1, \cdots N - 1$. It is important to note that in the current OFDM system with a non-large spreading code, K will always be equal to the length of the spreading code N. Therefore, the spread data for the current OFDM system can be derived from (1) as

$$D_{OFDM}(i) = \frac{1}{\sqrt{N}} \sum_{k=0}^{N-1} d(k) \cdot C(k, i). \tag{2}$$

On the other hand, in the MC-CDMA system, K is the number of active user that vary between 1 to K_{user}. Thus, the spread data for the MC-CDMA can be obtained from (1) as

$$D_{MC-CDMA}(i) = \frac{1}{\sqrt{K_{user}}} \sum_{k=0}^{K_{user}-1} d(k) \cdot C(k, i). \tag{3}$$

To simplify the presentation in this paper, we will use the term $D(i)$ as in (1) to express both the spread data $D_{OFDM}(i)$ and $D_{MC-CDMA}(i)$.

An oversampling is required to obtain an accurate result of the PAPR evaluation. In addition, a guard-band is practically used to reduce the adjacent channel interference (ACI) such as in IEEE.802.11a [21]. When the spreading code is CI or POCI code, the use of a guard-band (by nulling the unused subcarriers) results in a new system which is different from that pointed out in [22] and [23]. A signal with a guard-band and an oversampling can be obtained by performing a zero padding into the $D(i)$ to get D_{zp} as

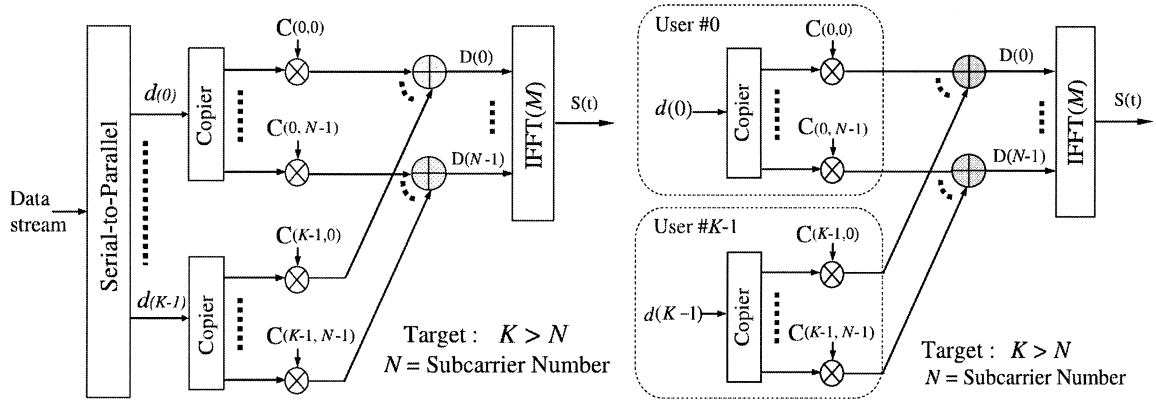

(a) The transmitter of an OFDM system with aspreading code. (b) The transmitter of a MC-CDMA system.

Fig. 1 The transmitter structures of an OFDM system with a spreading code and an MC-CDMA system.

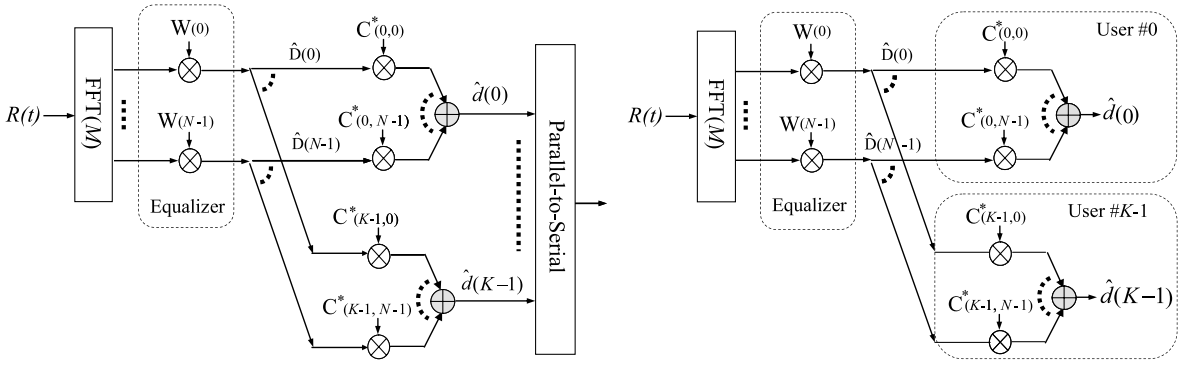

(a) The receiver of an OFDM system with a spreading code. (b) The receiver of a MC-CDMA system.

Fig. 2 The receiver structures of the OFDM system with spreading code and the MC-CDMA system.

$$D_{zp} = [\underbrace{D(0)\, D(1) \cdots D(\tfrac{N}{2}-1)}_{N/2} \underbrace{0\, 0\, \cdots 0}_{L} \underbrace{D(\tfrac{N}{2}) \cdots D(N-1)}_{N/2}], \tag{4}$$

where $M = L + N$ is the IFFT size. The n-th component of the zero-padded spread data D_{zp} is noted as $D_{zp}(n)$, where $n = 0, 1, \cdots, M-1$.

The spread data D_{zp} are then converted to a time domain by the IFFT with a size of M to obtain a time-discrete transmit signals (baseband)

$$S(t) = \frac{1}{\sqrt{M}} \sum_{n=0}^{M-1} D_{zp}(n) \cdot e^{j\left(\frac{2\pi}{M} \cdot t \cdot n\right)}, \tag{5}$$

where $t = 0, 1, \cdots, M-1$. The GI with cyclic extension [1] is then added to the signal $S(t)$.

We assume a slowly varying Rayleigh fading as the considered fading model. We also assume that the synchronization is perfectly carried out. It is also assumed that the delay spreading is less than the GI length in order to maintain the orthogonality amongst the subcarriers.

Figures 2(a) and 2(b) show the receiver structure of the OFDM system with a spreading code and the MC-CDMA system, respectively. Accompanied by the noise, the received signal $R(t)$ is expressed as

$$\begin{aligned} R(t) &= \widehat{S}(t) + \eta(t) \\ &= \frac{1}{\sqrt{M}} \sum_{n=0}^{M-1} H(n) \cdot D_{zp}(n) \cdot e^{j\left(\frac{2\pi}{M} \cdot t \cdot n\right)} + \eta(t), \end{aligned} \tag{6}$$

where $\widehat{S}(t)$ is the multipath faded signal $S(t)$, $H(n)$ is the channel impulse response (CIR) of the n-th subcarrier (will be cancelled by the equalizer) and $\eta(t)$ is the noise. Signal $R(t)$ is performed by the FFT to obtain the frequency domain signals $\widehat{D}(r)$

$$\begin{aligned} \widehat{D}(r) &= \frac{1}{\sqrt{M'}} \sum_{t=0}^{M'-1} R(t) \cdot e^{-j\left(\frac{2\pi}{M'} \cdot r \cdot t\right)} \\ &= \frac{1}{\sqrt{M'}} \sum_{t=0}^{M'-1} \left(\frac{1}{\sqrt{M}} \sum_{n=0}^{M-1} H(n) \cdot D_{zp}(n) \cdot e^{j\left(\frac{2\pi}{M} \cdot r \cdot n\right)} + \eta(t) \right) \\ &\quad \cdot e^{-j\left(\frac{2\pi}{M'} \cdot t \cdot r\right)} \\ &= H(r) \cdot D_{zp}(r) + Z(r), \end{aligned} \tag{7}$$

where $r = 0, 1, \cdots, M'-1$, M' is the size of FFT and $Z(r) = \frac{1}{\sqrt{M}} \sum_{t=0}^{M'-1} \eta(t) \cdot e^{-j\left(\frac{2\pi}{M'} \cdot t \cdot r\right)}$ is the noise. The useful subcarrier components can be obtained as (8), where $i = 0, 1, \cdots, N-1$.

$$\widehat{D}(i) = H(i) \cdot D(i) + Z(i) \tag{8}$$

This $\widehat{D}(i)$ signal is then equalized with weight values $W(i)$. We select minimum mean square error (MMSE) equalizer [2], a sub-optimal method for a performance which is close to maximum likelihood (ML) method on the multipath fading channel. As shown in Fig. 1, the MMSE equalization is located just after the FFT rather than between the de-spreading and the combiner as in [15]. Therefore, the computational complexity of the proposed structure is similar to the equalization of OFDM systems. The conventional structure in [15] may increase the computation complexity because of $K \times N$ complex multiplications should be performed.

Weighting values are derived from the MMSE criteria as

$$W(i) = \frac{H^*(i)}{|H(i)|^2 + \sigma}, \tag{9}$$

where $H^*(i)$ is the complex conjugate of the CIR $H(i)$, and σ is the variance of noise. We assume the σ is uniform over the all subcarriers.

The MMSE equalized signals are then de-spread using the complex conjugate $C^*(k,i)$ to obtain the received data $\widehat{d}(k)$ (as proven in the Appendix A)

$$\begin{aligned}\widehat{d}(k) &= \frac{1}{\sqrt{N}} \sum_{i=0}^{N-1} W(i) \cdot \widehat{D}(i) \cdot C^*(k,i) \\ &= \frac{1}{\sqrt{NK}} \sum_{i=0}^{N-1} \sum_{u=0}^{K-1} W(i) \cdot H(i) \cdot d(u) \cdot C(u,i) \cdot C^*(k,i) \\ &\quad + \frac{1}{\sqrt{N}} \sum_{i=0}^{N-1} W(i) \cdot Z(i) \cdot C^*(k,i). \end{aligned} \tag{10}$$

To simplify the presentation, it is assumed that the output of the equalizer is $Y(i) = W(i) \cdot H(i)$, while the element of the correlation of the spreading code is $X(u,k,i) = C(u,i) \cdot C^*(k,i)$. Thus, the (10) can be simplified as

$$\begin{aligned}\widehat{d}(k) &= \frac{1}{\sqrt{NK}} \sum_{i=0}^{N-1} \sum_{u=0}^{K-1} d(u) \cdot X(u,k,i) \cdot Y(i) \\ &\quad + \frac{1}{\sqrt{N}} \sum_{i=0}^{N-1} W(i) \cdot Z(i) \cdot C^*(k,i) \\ &= \frac{1}{\sqrt{NK}} \sum_{i=0}^{N-1} \sum_{u=0}^{K-1} d(u) \cdot X(u,k,i) \cdot Y(i) + \Gamma(k), \end{aligned} \tag{11}$$

where $\Gamma(k) = \frac{1}{\sqrt{N}} \sum_{i=0}^{N-1} W(i) \cdot Z(i) \cdot C^*(k,i)$ is the noise. From (11), we conclude that the element of the correlation $X(u,k,i)$ should be minimized when $u \neq k$.

3. The Proposed Large Spreading Code

A large spreading code with a larger code-number than its code-length is interesting in the view point of a spreading code design. Some examples of the current existing codes for class of large code are TOCS, quadriphase code, POGC and POCI code. Our new design has two purposes i.e. (1) provides a larger number of codes with a uniform low cross-correlation properties and (2) has an ability to reduce the PAPR level.

To satisfy the low PAPR level, the code is designed in a complex form with phase $\theta \in [0, 2\pi]$ and has energy of unity. The code is then generally constructed as

$$C(k,n) = e^{j\theta(k,n)}. \tag{12}$$

The next problem is how to select the best phase $\theta(k,n)$ to satisfy the correlation properties of a good code i.e. low cross-correlation (by keeping that auto-correlation is always 1.0). By redefining the element of the correlation $X(u,k,i)$ in (11) as $X(p,q,n) = C(p,n)C^*(q,n)$. The real part of the correlation for N subcarriers can be derived (as proven in Appendix B) as

$$\begin{aligned}\rho(p,q) &= \frac{1}{N} \sum_{n=0}^{N-1} C(p,n) \cdot C^*(q,n) \\ &= \frac{1}{N} \sum_{n=0}^{N-1} (\cos n\Delta\theta + j \sin n\Delta\theta) \\ &= \frac{1}{N} \left(\cos\{(N+1)\tfrac{1}{2}\Delta\theta\} + j \sin\{(N+1)\tfrac{1}{2}\Delta\theta\}\right) \\ &\quad \cdot \left(\frac{\sin \frac{1}{2}N\Delta\theta}{\sin \frac{1}{2}\Delta\theta}\right), \end{aligned} \tag{13}$$

where the integers $p, q \in [1, K_{max}]$ and $\Delta\theta = \theta(p, q+n) - \theta(p+n, q)$. The auto-correlation is obtained when $p = q$, noted as $\rho(p,p)$, i.e. $\rho(p,p) = \frac{1}{N} \sum_{n=1}^{N} (\cos n \cdot 0 + j \sin n \cdot 0) = N/N = 1$, while the cross-correlation is obtained with $p \neq q$ and noted as $\rho(p,q)$.

To obtain a good spreading code, the cross correlation $\rho(p,q)$ should be minimized. Phases for a perfect orthogonality $\rho(p,q) = 0$ can be obtained easily by solving (13) i.e. phases of $\sin \frac{1}{2}N\Delta\theta = 0$ by keeping $\sin \frac{1}{2}\Delta\theta \neq 0$. Finally, we will get $\Delta\theta = \frac{2\pi}{N}$ which is the basic phases of Carrier Interferometry (CI) code. However, it does not meet our purpose to increase the capacity to $K > N$ because the number of different phases is equal to the number of subcarriers. Consequently, it results in a spreading codes with size of $N \times N$. Figure 3 plots the real and imaginary parts of (13) for subcarrier $N = 4$. It is shown that the CI code has 4 phases with zero correlations.

In this paper, we consider the binary phase shift keying (BPSK) symbols. Therefore, it is acceptable to consider only the real parts of (13) in this paper. Code design that considers real and imaginary parts is left for future work. Thus, now we only focus on the real parts of (13). Let us note the real parts of $\rho(p,q)$ in (13) with $R(p,q)$ as

$$\begin{aligned}R(p,q) &= \mathrm{Re}\{\rho(p,q)\} \\ &= \frac{1}{N} \cos (N+1)\, \tfrac{1}{2}\Delta\theta \cdot \frac{\sin \frac{1}{2}N\Delta\theta}{\sin \frac{1}{2}\Delta\theta} \end{aligned}$$

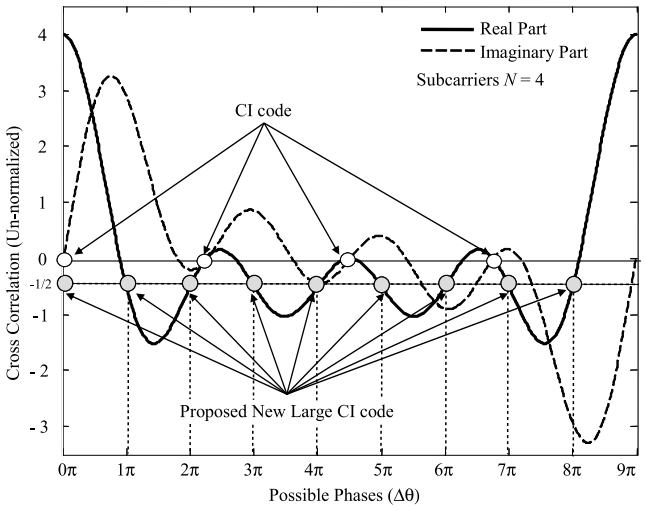

Fig. 3 The real parts and imaginary parts of the correlation $X(p, q)$ of the proposed LCI code.

$$= \frac{1}{N}\left(\frac{\sin(2N+1)\frac{1}{2}\Delta\theta}{2\sin\left(\frac{1}{2}\Delta\theta\right)} - \frac{1}{2}\right). \tag{14}$$

By allowing the cross-correlation in (14) to be $R(p, q) = |-\frac{1}{2N}|$ (because it is reasonable to get low cross-correlation which is close to $R(p, q) \approx 0$ for a large N) and by keeping $\sin\left(\frac{1}{2}\Delta\theta\right) \neq 0$, we can obtain new phases that satisfy $R(p, q) = |-\frac{1}{2N}|$ by solving

$$\frac{\sin(2N+1)\frac{1}{2}\Delta\theta}{2\sin\left(\frac{1}{2}\Delta\theta\right)} = 0. \tag{15}$$

The phases that satisfy the equality in (15) are

$$(2N+1)\frac{1}{2}\Delta\theta = \pi k,\ k = 0, 1, \cdots, 2N. \tag{16}$$

The value of k is limited to $2N$ because the $\sin(2N+1)\frac{1}{2}\Delta\theta$ is an alias of $\sin\frac{1}{2}\Delta\theta$ when $k > 2N$. Now, we obtain new $(2N+1)$ phases (phase 0 is included) for N subcarriers as

$$\Delta\theta = \frac{2\pi k}{(2N+1)}. \tag{17}$$

As an example for a number of subcarriers $N = 4$, we get 9 phases with an equal space as illustrated in Fig. 3 i.e. $\{0, 1, 2, 3, 4, 5, 6, 7, 8\} \times \frac{2\pi}{9}$.

Finally, from (12) and (A· 3) that shows the considered n from $n = 0, \cdots, N-1$ to $n = 1, \cdots, N$, the proposed code can be constructed as

$$C(k, n) = e^{j\left(\frac{2\pi}{2N+1}\right)\cdot k\cdot(n+1)}, \quad \text{for} \begin{cases} k = 0, 1, \cdots 2N \\ n = 0, 1, \cdots N-1 \end{cases}. \tag{18}$$

Equation (18) shows that the proposed code has a code-number of $(2N+1)$ while its code-length is N. Consequently, the size is becoming $(2N+1)\times N$. Now, the designed spreading code meets the condition of code where its code-number is larger than its code-length. It means that user capacity can be extended up to $(2N + 1)$ users for the multiuser multicarrier system with N subcarriers. In the OFDM system, $(2N + 1)$ data symbols can be assigned on N subcarriers.

4. Cross Correlations Analysis

This section analyzes the cross-correlation of the proposed LCI code and the POCI code. As discussed in the previous section, a code with uniform/equal cross-correlations is interesting because of its assurance in the linearly independent set that provide a minimum BER degradation. A code is said to have a uniform cross-correlation if the cross-correlation between different signals are all equal so we have the correlation matrix of that code as

$$R = \begin{bmatrix} 1 & & & \\ & 1 & \varphi & \\ & & \ddots & \\ & \varphi & & 1 \\ & & & 1 \end{bmatrix}. \tag{19}$$

The matrix has all elements on the main diagonal are equal to unity while the other parts equal to φ. It was also proven in [18] that this matrix has only two distinct eigenvalues i.e. $1 - \varphi$ and $1 + (K-1)\varphi$ for a matrix with a size of $K \times K$. Consequently, the value of φ is in the range of

$$-\frac{1}{K-1} \leq \varphi \leq 1, \tag{20}$$

where, K is the code-number. Recalling (14), the cross correlation of the proposed LCI code with its equal cross-correlation can be formulated as

$$R_{LCI}(p, q) = \begin{cases} 1, & \text{for} \quad p = q \\ |-\frac{1}{2N}|, & \text{for} \quad p \neq q \end{cases}. \tag{21}$$

Here, we find that $\varphi = -\frac{1}{2N}$ for $K = 2N + 1$. Now, it is clear that (20) can be satisfied by the proposed LCI code.

The POCI code for N subcarriers comprises two code sets of the CI code (phase $\frac{\pi}{N}\cdot n$ is added to the modify the second code set) as

$$POCI(k, n) = \begin{cases} e^{j\left(\frac{2\pi}{N}\cdot k\cdot n\right)}, \\ \text{for } k = 0, 1, \cdots, N-1 \\ \\ e^{j\left(\frac{2\pi}{N}\cdot k\cdot n + \frac{\pi}{N}\cdot n\right)}, \\ \text{for } k = N, N+1, \cdots, 2N-1 \end{cases}. \tag{22}$$

The cross-correlation in each code set is zero but not for that of between the code sets. The non-zero cross-correlation appears when $p > N, q \leq N$ or $q > N, p \leq N$. Appendix C carefully derived the cross-correlation of real and imaginary parts of the POCI codes. With the same assumption that the data symbols are in BPSK, we only focus on the real components of the cross-correlations. The real part of cross-correlation of the POCI code (as proven in Appendix C) can

be described as

$$R_{POCI} = \frac{1}{N}\left(\frac{1}{2} + \frac{\sin\left(\left(N-\frac{1}{2}\right)\left(\frac{2\pi}{N}k+\frac{\pi}{N}\right)\right)}{2\sin\left(\frac{1}{2}\left(\frac{2\pi}{N}k+\frac{\pi}{N}\right)\right)}\right)$$
$$= \frac{1}{N}\left(\frac{1}{2} + \frac{\begin{array}{c}\sin(2\pi k+\pi)\cos\left(\frac{1}{2}\left(\frac{2\pi}{N}k+\frac{\pi}{N}\right)\right)\\ -\cos(2\pi k+\pi)\sin\left(\frac{1}{2}\left(\frac{2\pi}{N}k+\frac{\pi}{N}\right)\right)\end{array}}{2\sin\left(\frac{1}{2}\left(\frac{2\pi}{N}k+\frac{\pi}{N}\right)\right)}\right)$$
(Here for any integer k, $\sin(2\pi k+\pi) = 0$ and $\cos(2\pi k+\pi) = -1$)
$$= \frac{1}{N}\left(\frac{1}{2}+\frac{1}{2}\right), \quad (23)$$

and generally as

$$R_{POCI}(p,q) = \begin{cases} 1, & \text{for } p = q \\ 0, & \text{for } p \neq q,\ p,q \in [0, N-1] \\ & \leftrightarrow p,q \in [N, 2N-1] \\ \frac{1}{N}, & \text{otherwise} \end{cases}. \quad (24)$$

Now, we can compare the cross-correlation of the proposed LCI in (21) and the POCI codes in (24). For an example with $N = 4$, Fig. 4 illustrates shapes of the correlation of LCI and POCI codes. We can fairly compare the orthogonality of both codes using this figure. POCI codes 1 up to 4 are correlated to code 5 up to 8 (indicated by a gray area), while the proposed LCI code has lower and equal correlations with code 5 up to 9 (indicated by similar white color that covers the whole area). It means that the proposed LCI code is capable of providing low and uniform cross-correlations which ensure user fairness and lower error probability.

Revisiting (21) and (24), we get the maximum cross-correlation R_{max} of the POCI and the proposed LCI codes as

$$I_{max}(POCI) = \sqrt{\frac{1}{N}}, \quad (25)$$

and

$$I_{max}(LCI) = \sqrt{\frac{1}{2N}}. \quad (26)$$

to $N = 32$. It can be observed that for any value of N the R_{max} of the proposed LCI code is always equal to half of the cross-correlation of the POCI code. For $N = 16$, we get $R_{max}(LCI) = \sqrt{\frac{1}{2N}} = 0.1768$ while $R_{max}(POCI) = \sqrt{\frac{1}{N}} = 0.2500$.

5. PAPR and Instantaneous Normalized Power Evaluations

The superposition of N signals to obtain the OFDM symbol may generate a high peak signal level. The PAPR is obtained by taking into account only one sample (the highest peak) per OFDM symbol. From a practical point of view, however, it is not interesting to evaluate only one sample of that maximum peak, but investigating all samples will give a better evaluation to the peak power distributions. Therefore, beside the PAPR evaluation we present an instantaneous normalized power (INP) performance to describe the power distribution in all samples.

The PAPR is mathematically measured as

$$PAPR = 10\log_{10}\left(\left\{\frac{\max(|S(t)|^2)}{\mathrm{E}[|S(t)|^2]}\right\}_{0\le t<M-1}\right)\mathrm{dB}, \quad (27)$$

where $E[\cdot]$ is the average of the power signal $|S(t)|^2$, while $S(t)$ and M is the length of OFDM symbol and FFT size as defined in (5), respectively. When the PAPR measures one sample per OFDM symbol, the INP measures all generated samples in an OFDM symbol. The INP is mathematically expressed as

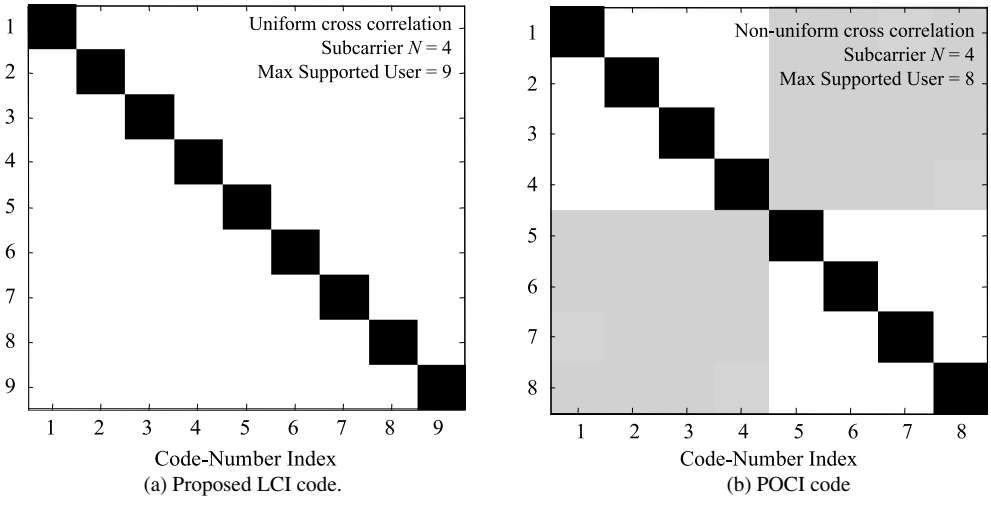

Fig. 4 Cross Correlation's shape of (a) the proposed LCI code and (b) the POCI code.

$$INP = 10\log_{10}\left(\left\{\frac{|S(t)|^2}{E[|S(t)|^2]}\right\}_{0\le t<M-1}\right)\text{dB}. \quad (28)$$

The superpositions of signals that cause a high PAPR level are expected to be avoided by employing a complex spreading code. To meet this condition, the code should be composed of complex components with phases $\theta \in [0, 2\pi]$ and energy of unity. Thus, the proposed code which was designed to satisfy this condition will be evaluated in this section.

We consider OFDM and MC-CDMA with the number of subcarriers $N = 16$ and BPSK symbols. As a consequence, the code-length of the POCI and the proposed LCI codes is equal to 16, while the code-number of POCI and proposed LCI code is 32 and 33, respectively. It means that in one OFDM symbol with the POCI code, 32 BPSK symbols can be assigned, while in one OFDM symbol with LCI code 33 BPSK symbols are able to be assigned. With $N_{OS} = 10,000$ OFDM symbols, we plot the PAPR and INP performances of both POCI and LCI codes. Considering the oversampling factor $L = 4$, the obtained samples in the the INP analysis are about 10^5 samples.

The results of PAPR evaluations are plotted in Fig. 5 for a complementary cumulative distribution function (CCDF) of 10^{-4}. CCDF of 10^{-4} means that the probability of PAPR exceeds a determined value (shown in its abscissa) is 10^{-4}. It is shown that the PAPR level of OFDM is about 11.5 dB, while the OFDM with the POCI code is 7.5 dB. Thus, a significant reduction about 4 dB is obtained. It is interesting to note that the proposed LCI code also achieved a similar PAPR performance with that of the POCI code about 7.5 dB at CCDF of 10^{-4}.

Figure 5 shows the INP performances of OFDM with the POCI and LCI codes and that of OFDM without spreading code. At CCDF of 10^{-4} the INP of OFDM is more than 10 dB, while the INP of POCI and the proposed LCI codes are similar in about 7.2 dB. The proposed LCI code has a similar performance as that of the POCI code for both in the PAPR and the INP performances because the LCI has been constructed from complex elements with phase $\theta \in [0, 2\pi]$ and energy of unity. Here, we can conclude that the proposed spreading code is capable of reducing significantly the PAPR and the INP of the OFDM system similar as that of with the POCI code.

In the MC-CDMA system which whose performance of peaks power depends on the number of active users, we prefer to investigate the peaks with PAPR rather than the INP performances for the reason of simplicity since PAPR only measures the maximum power. The results of the PAPR performances are shown in Fig. 6 for several number of active users. The result was obtained from 10,000 MC-CDMA symbols (downlink) with number of active users is varied from 1 to 32 for POCI and 1 to 33 for the proposed LCI code. The PAPR performance of the proposed LCI and the POCI codes is very similar for any number of active users, where both the PAPR of the POCI and the LCI codes decrease as the number of active users increases.

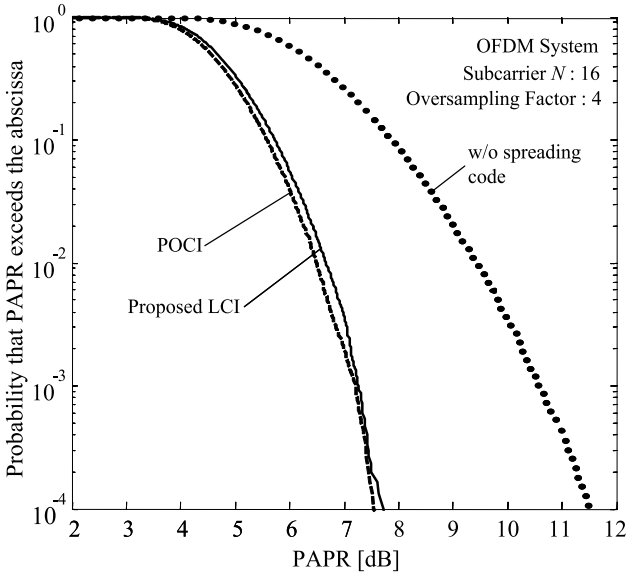

(a) PAPR performance.

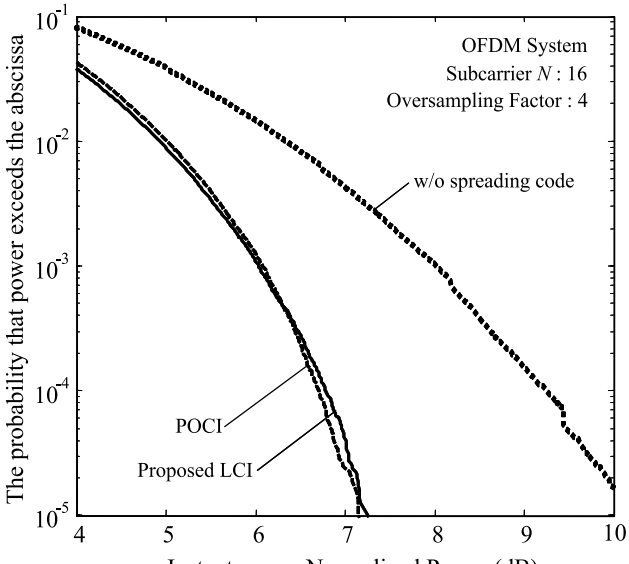

(b) INP performance.

Fig. 5 PAPR and Instantaneous Normalized Power (INP) performances of OFDM signals using POCI and the proposed LCI code.

6. BER Performances Evaluation

This section evaluates the BER performance of the proposed LCI code in the additive-white Gaussian noise (AWGN) and a multipath fading channel for both OFDM and MC-CDMA systems with parameters as shown in Table 1.

6.1 The BER in AWGN Channel

We evaluate the BER performance of the OFDM system with the number of subcarriers $N = 16$. It means that one OFDM symbol contains 32 BPSK data symbols for the POCI code and 33 BPSK data symbols for the proposed

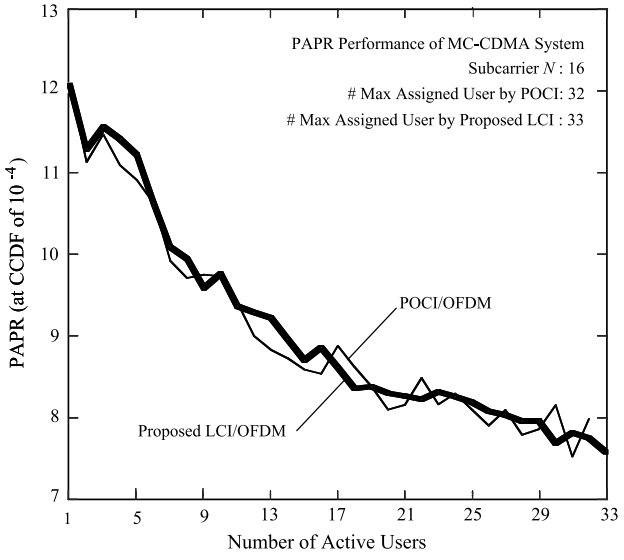

Fig. 6 PAPR performance of MC-CDMA signals using POCI and the proposed LCI code.

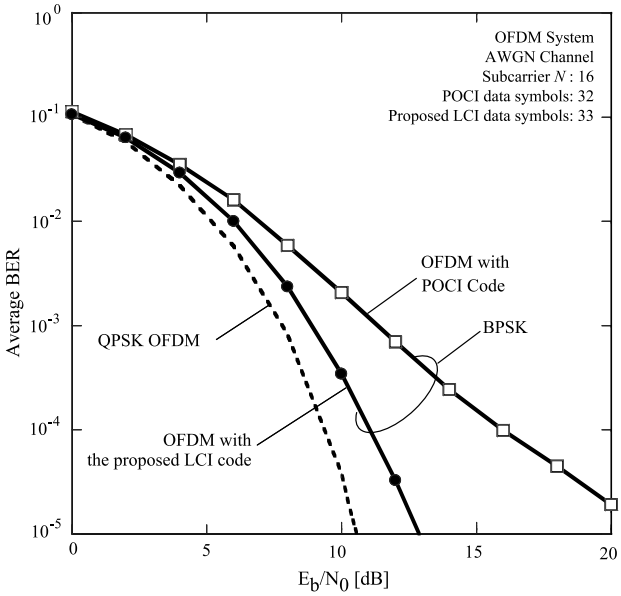

Fig. 7 The BER performance of POCI and the proposed LCI code in the AWGN channel.

Table 1 Simulation parameters.

Parameters	Values
Modulation and Spreading Code ($C(k,n)$)	BPSK ⇒ POCI BPSK ⇒ Proposed LCI QPSK ⇒ OFDM (without spreading code)
Code-Length	16
Subcarrier (N)	16
Oversampling Factor (OSF)	4
Zero Padding (L)	(OSF-1)×N
Guard Interval Length	25% of OFDM symbol's length
Error Correction Coding	Convolutional Coding Code rate $r = 1/2$ and $r = 2/3$
Channel Model	AWGN Bad Urban COST-207 [24]
Channel estimation Equalizer	Perfect MMSE

LCI code. For a fair comparison, we also plot the BER performance of quadrature phase shift keying (QPSK) symbols in OFDM (without spreading code) by expecting that the number of information bits in OFDM transmission is similar i.e. 32 bits with QPSK, 32 bits with POCI and 33 bits with the proposed LCI code. The results are plotted in Fig. 7. Though the LCI code has a BER degradation about 1.4 dB compared with that of QPSK OFDM, the LCI code outperforms the POCI code about 5 dB at an average BER of 10^{-4}. This improvement comes from the benefit of the uniform cross-correlation $\varphi = |-\frac{1}{2N}|$ presented by the proposed LCI code. However, the degradation of the LCI code when compared with the QPSK, comes from the non-zero cross-correlation of LCI code especially when N is small. We expect that the degradation diminish as the number of subcarriers N increases, because $\varphi = |-\frac{1}{2N}| \simeq 0$ for a large N.

6.2 The BER in a Multipath Fading Channel

In the multipath fading environment evaluation, we evaluated the OFDM with subcarrier $N = 16$. BPSK data symbol is considered for the POCI and the LCI, while QPSK data symbol is for the OFDM without spreading code to guarantee a fair capacity comparison. For the MC-CDMA evaluation, we plot the BER with two numbers of active users i.e. below $N(K_{user} = 10)$ and above N ($K_{user} = 30$).

Figure 8 shows the BER of the OFDM system versus the E_b/N_0. Three curves are presented i.e. the BER of OFDM without spreading code, with POCI code and with the proposed LCI codes. From the figure, we can conclude that the code has gain about 3.6 dB compared with the POCI code and 7.5 dB compared with QPSK OFDM (without a spreading code) at an average BER of 10^{-4}. It can be concluded that the LCI spreading code provides advantages in multipath fading channel than the POCI and QPSK OFDM without a spreading code.

For the MC-CDMA system, with the same fading model, BER performance results are plotted in Fig. 9 for a several numbers of users $K_{user} = 10$ (load factor of 62%) and 30 (load factor of 188%). When the $K_{user} = 10$, it is observed that the POCI and the LCI code has a similar performance. It is interesting to note that the proposed LCI code with the uniform cross-correlation of $\varphi = |-\frac{1}{2N}|$ provides a similar performance as that of the POCI, though when $K_{user} \leq N$, the POCI may have cross-correlation $\varphi = 0$ (orthogonal in parts). However, the BER performance of the POCI code degrades as the number of active users increases above 16 users ($K_{user} > N$). $K_{user} > N$ is the condition when the POCI code becomes completely un-orthogonal with the cross-correlation $\varphi = \frac{1}{N}$. For $K_{user} = 30$, the proposed

code improves BER performance about 2.8 dB at the average BER of 10^{-4}.

6.3 The BER in the Presence of Error Correction Coding

This section evaluates the performance when the error correction coding is employed. A convolutional coding with coding rate $r = 1/2$ and $r = 2/3$ is employed. The convolutional encoder has a constraint length $K = 7$ with a generator polynomials in octal representation is [171,133].

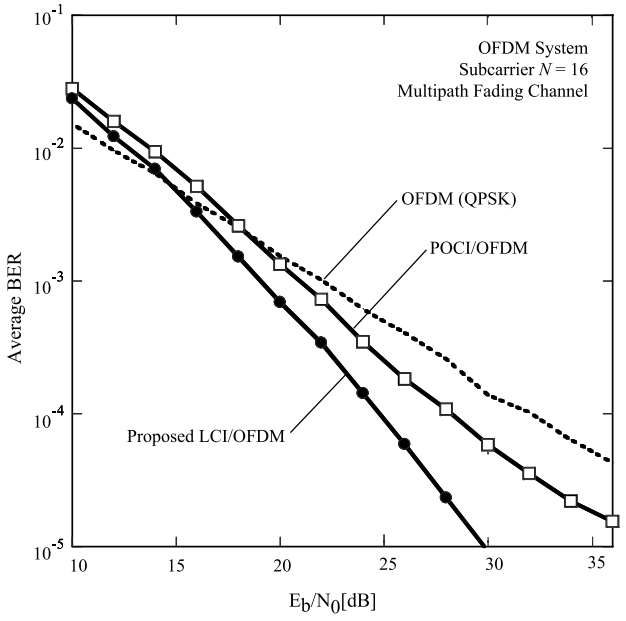

Fig. 8 The BER performance of OFDM with POCI and the proposed LCI code in a multipath fading channel.

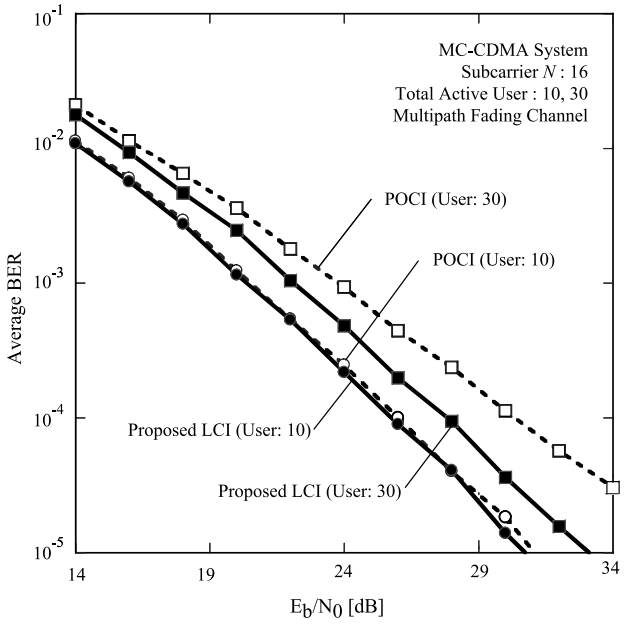

Fig. 9 The BER performance of MC-CDMA with POCI and the proposed LCI code in multipath fading channel.

Though, the evaluation is performed for the OFDM system, the MC-CDMA system is expected to have the same trend as the results in OFDM system.

Figure 10 plotted the BER performance in the AWGN and multipath fading channel. As shown in Fig. 10(a), with a coding rate $r = 2/3$, the proposed LCI code provides the best performance even with the QPSK in OFDM system. When the coding rate is set to $r = 1/2$, the proposed LCI code has a small degradation compared with OFDM and the POCI code.

Figure 10(b) plotted the BER in multipath fading channel. For a code rate $r = 1/2$, the proposed LCI code has

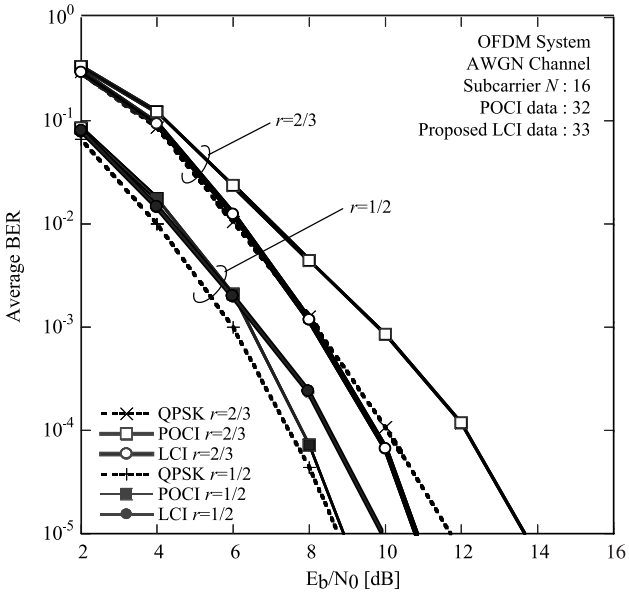

(a) BER in AWGN.

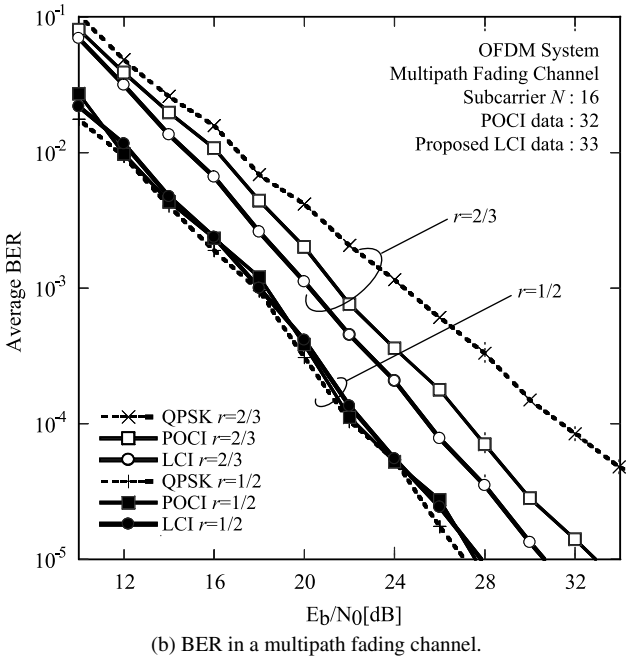

(b) BER in a multipath fading channel.

Fig. 10 BER performances of the coded system with coding rate $r = 1/2$ and $r = 2/3$.

a similar performance with the POCI and QPSK OFDM systems. However, with $r = 2/3$, the proposed LCI code has the best performance about 2.5 dB and 1 dB better compared with the BER performance of QPSK OFDM and POCI/OFDM at sthe BER of 10^{-4}, respectively.

Finally, we conclude that the BER performances in the presence of error correction has a similar trend with the derivation in [3] i.e. a coded spread OFDM outperforms a coded OFDM for code rate $r > 1/2$, while there is no significant difference when the code rate $r < 1/2$. An explanation of this phenomenon is that the high redundancy of low code rates (associated with interleaving) already performs a kind of spreading by linking a number of subcarriers through the memory introduced by the convolutional encoder. It exploits all the diversity of the channel.

7. Conclusions

We have introduced a new large complex spreading code set, called as LCI code, for OFDM and MC-CDMA systems which is capable of supporting $(2N + 1)$ users and data symbols over the N subcarriers with better performances than the current POCI code. The LCI code provides a uniform low cross-correlation which is required to distinguish the data/users with minimum probability of errors. The cross-correlation of the proposed LCI code is half of that of the POCI code. In term of the PAPR performance, the results confirm that the proposed LCI code has a similar PAPR performance with that of the POCI code. The BER performance of the proposed LCI in OFDM system is about 5 dB and 3.6 dB better than that of the POCI codes in the AWGN and a multipath fading channels, respectively. In the presence of error correction coding with a coding rate larger than 1/2, the proposed LCI code provides a better performance about 2.5 dB and 1 dB than the coded QPSK OFDM and the coded POCI/OFDM. For the MC-CDMA system, the BER performance of the proposed LCI code is similar to that of the POCI when the load factor is less than 100%. When the load factor increases more than 100%, the improvement of the LCI code is about 3.8 dB at the load factor of 188%. Another important issue for spreading code implementation is their computational complexity. Unfortunately, we could not present it in this paper. We decided to evaluate the computational complexity of the proposed code in the future work. In addition, the future work will focus on the complex modulations (such as QPSK and M-QAM modulation) by taking into account the imaginary parts of the cross-correlation.

Acknowledgments

The authors would like to thank JSAT Corp., Japan, for supporting this research.

References

[1] R.V. Nee and R. Prasad, OFDM for Wireless Multimedia Communications. Artech House Publisher, 2001.

[2] S. Hara and R. Prasad, "Overview of multicarrier CDMA," IEEE Commun. Mag., vol.35, no.12, pp.126–133, Dec. 1997.

[3] M. Debbah, P. Loubaton, and M. de Courville, "Spread OFDM performance with MMSE equalization," IEEE International Conference on Acoustics, Speech, and Signal Processing (ICASSP), vol.4, pp.2385–2388, May 2001.

[4] N. Yee, P. Linnartz, and G. Fettweis, "Multi-carrier CDMA in indoor wireless networks," IEICE Trans. Commun. (Japanese Edition), vol.J77-B, no.7, pp.900–904, July 1994.

[5] A. Bury, J. Eagle, and J. Lindner, "Diversity comparison of spreading transforms for multicarrier spread spectrum transmission," IEEE Trans. Commun., vol.51, no.5, pp.774–781, May 2003.

[6] D.A. Wiegandt, C.R. Nassar, and Z. Wu, "Overcoming peak-to-average power ratio issues in OFDM via carrier interferometry codes," IEEE Vehicular Technology Conferece (VTC), pp.660–663, Atlantic City, NJ, May 2001.

[7] K. Anwar, M. Saito, T. Hara, M. Okada, and H. Yamamoto, "Simplified realization of carrier interferometry ofdm by FFT algorithm," IEEE VTS Asia Pacific Wireless Communications Symposium (APWCS), pp.199–203, Aug. 2005.

[8] K. Anwar, M. Saito, H. T, M. Okada, and H. Yamamoto, "Simplified realization of pseudo-orthogonal carrier interferometry ofdm by FFT algorithm," in Multicarrier Spread Spectrum from IEEE Multi-Carrier Spread Spectrum (MC-SS) Khaled Fazel, ed. S. Kaiser, 2006, Hardcover, ISBN:1-4020-4435-6, pp.167–174, Oberpfaffenhofen, Germany, 2005.

[9] K. Anwar and H. Yamamoto, "A new design of carrier interferometry OFDM with FFT as spreading codes," IEEE Radio and Wireless Symposium (RWS), pp.543–546, San Diego, CA, Jan. 2006.

[10] K. Anwar, M. Saito, T. Hara, M. Okada, and H. Yamamoto, "On the PAPR reduction of wavelet-based multicarrier modulations system," IASTED Communications and Computer Network (CCN), pp.138–143, MIT, CA, USA, 2004.

[11] F. Vanhaverbeke, M. Moeneclay, and H. Sari, "DS/CDMA with two sets of orthogonal spreading sequences and iterative detection," IEEE Commun. Lett., vol.4, no.9, pp.289–291, 2000.

[12] B.M. Popovic, N. Suehiro, and P.Z. Fan, "Orthogonal sets of quadriphase sequences with good cross correlation properties," IEEE Trans. Inf. Theory, vol.48, no.4, pp.956–959, 2002.

[13] B. Natarajan, C.R. Nassar, S. Shattil, M. Michelini, and Z. Wu, "High-performance MC-CDMA via carrier interferometry codes," IEEE Trans. Veh. Technol., vol.50, no.6, pp.1344–1353, Nov. 2001.

[14] B. Natarajan, Z. Wu, C.R. Nassar, and S. Shatill, "Large set of CI spreading codes for high capacity mc-cdma," IEEE Trans. Commun., vol.52, no.11, pp.1862–1866, Nov. 2004.

[15] D.A. Wiegandt, Z. Wu, and C.R. Nassar, "High-throughput, high-performance OFDM via pseudo-orthogonal carrier interferometry spreading codes," IEEE Trans. Commun., vol.51, no.7, pp.1123–1134, July 2003.

[16] K. Anwar, "Peak-to-average power ratio reduction of OFDM signals using carrier interferometry codes and iterative processing," Master's thesis, Nara Institute of Science and Technology, March 2005. (available at http://shika.aist-nara.ac.jp/member/anwar-k/download/mthesis_k_anwar.pdf)

[17] N. Taylor, M.A. Cooper, S.M. D. Armour, and G.P. McGeehan, "Performance evaluation of carrier interferometry implementations of mc-cdma over a wideband channel suffering phase noise," IEEE Veh. Technol. Conference Spring, vol.5, pp.3043–3047, June 2005.

[18] J. Max, "Signal set with uniform correlation properties," the Society for Industrial and Applied Mathematics, vol.10, pp.113–118, March 1962.

[19] G. Chandran and J.S. Jaffe, "Signal set design with constrained amplitude spectrum and specified time-bandwidth product," IEEE Trans. Commun., vol.44, no.6, pp.725–732, June 1996.

[20] P. Xia, S. Zhou, and G.B. Giannakis, "Achieving the welch bound with difference sets," IEEE Trans. Inf. Theory, vol.51, no.5, pp.1900–1907, May 2003.

[21] IEEE.802.11a-1999, High Speed physical layer in the 5 GHz band, 1999.
[22] Y. Kuang, K. Long, C. Wu, and Q. Chen, "Comments on high-througput high performance OFDM via pseudo-orthogonal carrier interferometry spreading codes," IEEE Trans. Commun., vol.55, no.1, pp.232–234, Jan. 2007.
[23] J. lei and L. Wu, "Comments on high-througput high performance ofdm via pseudo-orthogonal carrier interferometry spreading codes," IEEE Trans. Commun., vol.55, no.5, p.1088, May 2007.
[24] M. Patzold, Mobile Fading Channels, John Wiley & Sons, 2002.

Appendix A: Proof of Equation (10)

$$\begin{aligned}
\widehat{d}(k) &= \frac{1}{\sqrt{K}}\sum_{i=0}^{K-1} W(i)\cdot\widehat{D}(i)\cdot C^*(k,i)\\
&= \frac{1}{\sqrt{K}}\sum_{i=0}^{K-1} W(i)\cdot\{(H(i)\cdot D(i)+Z(i)\}\cdot C^*(k,i)\\
&\quad \text{(with } \widehat{D}(i) \text{ from (8))}\\
&= \frac{1}{\sqrt{K}}\sum_{i=0}^{K-1} W(i)\cdot H(i)\left(\frac{1}{\sqrt{K}}\sum_{u=0}^{K-1} d(u)\cdot C(u,i)\right)\\
&\quad \cdot C^*(k,i)\\
&\quad +\frac{1}{\sqrt{K}}\sum_{i=0}^{K-1} W(i)\cdot Z(i)\cdot C^*(k,i)\\
&\quad \text{(with } D(i) \text{ from (1) but } k \text{ in (1) is changed}\\
&\quad \text{to } u \text{ to avoid redundant parameters)}\\
&= \frac{1}{K}\sum_{i=0}^{K-1}\sum_{u=0}^{K-1} W(i)\cdot H(i)\cdot d(u)\cdot C(u,i)\cdot C^*(k,i)\\
&\quad +\frac{1}{\sqrt{K}}\sum_{i=0}^{K-1} W(i)\cdot Z(i)\cdot C^*(k,i). \qquad (\text{A}\cdot 1)
\end{aligned}$$

Appendix B: Proof of the Proposed Code's Correlation in Equation (13)

$$\begin{aligned}
\rho(p,q) &= \frac{1}{N}\sum_{n=0}^{N-1} C(p,n)\cdot C^*(q,n)\\
&= \frac{1}{N}\sum_{n=0}^{N-1} e^{j(\theta_{(p,n)}-\theta_{(q,n)})}\\
&= \frac{1}{N}\sum_{n=0}^{N-1} e^{j\cdot n\Delta\theta}; \quad (n\Delta\theta=\theta_{(p,n)}-\theta_{(q,n)}). \quad (\text{A}\cdot 2)
\end{aligned}$$

We are interested to design a code which its all elements are complex, therefore it is acceptable to change the index n from $n = 0, 1, \cdots, N-1$ to $n = 1, 2, \cdots, N$ of (A·2) and obtain

$$\rho(p,q) = \frac{1}{N}\sum_{n=1}^{N} e^{j\cdot n\Delta\theta}. \qquad (\text{A}\cdot 3)$$

Now it is becoming easy to be solved using Geometric series for the total summation up to N as

$$S_N = \frac{r(1-r^N)}{1-r}, \qquad (\text{A}\cdot 4)$$

where r is the ratio of the Geometric series. From (A·3), we got $r = e^{j\Delta\theta}$ to obtain

$$\begin{aligned}
\rho(p,q) &= \frac{1}{N}S_N\\
&= \frac{1}{N}\frac{e^{j\Delta\theta}(1-e^{j\Delta\theta\cdot N})}{1-e^{j\Delta\theta}}\\
&= \frac{1}{N}\frac{e^{j\frac{1}{2}\Delta\theta}(1-e^{j\Delta\theta\cdot N})}{e^{-j\frac{1}{2}\Delta\theta}-e^{j\frac{1}{2}\Delta\theta}}\\
&= \frac{1}{N}\frac{e^{j(N+1)\frac{1}{2}\Delta\theta}(e^{-j\frac{1}{2}\Delta\theta\cdot N}-e^{j\frac{1}{2}\Delta\theta\cdot N})}{e^{-j\frac{1}{2}\Delta\theta}-e^{j\frac{1}{2}\Delta\theta}}\\
&= \frac{1}{N}e^{j(N+1)\frac{1}{2}\Delta\theta}\cdot\left(\frac{e^{-j\frac{1}{2}\Delta\theta\cdot N}-e^{j\frac{1}{2}\Delta\theta\cdot N}}{e^{-j\frac{1}{2}\Delta\theta}-e^{j\frac{1}{2}\Delta\theta}}\right)\\
&= \frac{1}{N}\left(\cos\{(N+1)\tfrac{1}{2}\Delta\theta\}+j\sin\{(N+1)\tfrac{1}{2}\Delta\theta\}\right)\\
&\quad \cdot\left(\frac{\sin\frac{1}{2}N\Delta\theta}{\sin\frac{1}{2}\Delta\theta}\right). \qquad (\text{A}\cdot 5)
\end{aligned}$$

Appendix C: Proof of Equation (23)

POCI code has two distinct cross-correlations i.e. zero and non-zero (ψ) values as derived below. The zero cross-correlation exists if and only if $p, q \in [0, N-1]$ or $p, q \in [N, 2N-1]$. Generally, cross correlation of POCI can be derived as

$$\rho^{POCI}(p,q)\Big| = \begin{cases} 0, & p,q\in[0,N-1] \\ & \leftrightarrow p,q\in[N,2N-1] \\ \psi, & \text{otherwise} \end{cases} \qquad (\text{A}\cdot 6)$$

where

$$\begin{aligned}
\psi &= \frac{1}{N}\sum_{n=0}^{N-1} e^{j\left(\frac{2\pi}{N}k+\frac{\pi}{N}\right)\cdot n}\\
&= \frac{1}{N}\left(\frac{1-e^{j\left(\frac{2\pi}{N}k+\frac{\pi}{N}\right)\cdot N}}{1-e^{j\left(\frac{2\pi}{N}k+\frac{\pi}{N}\right)}}\right)\\
&= \frac{1}{N}\left(\frac{e^{-j\frac{1}{2}\left(\frac{2\pi}{N}k+\frac{\pi}{N}\right)}-e^{j\left(N-\frac{1}{2}\right)\left(\frac{2\pi}{N}k+\frac{\pi}{N}\right)}}{e^{-j\frac{1}{2}\left(\frac{2\pi}{N}k+\frac{\pi}{N}\right)}-e^{j\frac{1}{2}\left(\frac{2\pi}{N}k+\frac{\pi}{N}\right)}}\right)
\end{aligned}$$

$$
\begin{aligned}
&= \frac{1}{N}\left(\frac{e^{-j\frac{1}{2}\left(\frac{2\pi}{N}k+\frac{\pi}{N}\right)} - e^{j\left(N-\frac{1}{2}\right)\left(\frac{2\pi}{N}k+\frac{\pi}{N}\right)}}{-2j\sin\frac{1}{2}\left(\frac{2\pi}{N}k+\frac{\pi}{N}\right)}\right) \\
&= \frac{1}{N}\left(\frac{j\left(e^{-j\frac{1}{2}\left(\frac{2\pi}{N}k+\frac{\pi}{N}\right)} - e^{j\left(N-\frac{1}{2}\right)\left(\frac{2\pi}{N}k+\frac{\pi}{N}\right)}\right)}{2\sin\frac{1}{2}\left(\frac{2\pi}{N}k+\frac{\pi}{N}\right)}\right) \\
&= \frac{1}{N}\left(\frac{\sin\frac{1}{2}\left(\frac{2\pi}{N}k+\frac{\pi}{N}\right)+\sin\left(\left(N-\frac{1}{2}\right)\left(\frac{2\pi}{N}k+\frac{\pi}{N}\right)\right)}{2\sin\frac{1}{2}\left(\frac{2\pi}{N}k+\frac{\pi}{N}\right)}\right) \\
&\quad + j\cdot\frac{1}{N}\left(\frac{\cos\frac{1}{2}\left(\frac{2\pi}{N}k+\frac{\pi}{N}\right)-\cos\left(\left(N-\frac{1}{2}\right)\left(\frac{2\pi}{N}k+\frac{\pi}{N}\right)\right)}{2\sin\frac{1}{2}\left(\frac{2\pi}{N}k+\frac{\pi}{N}\right)}\right)
\end{aligned}
\tag{A·7}
$$

$R_{POCI}(p,q)$ is taken from the real parts of the above equation as

$$
\begin{aligned}
R_{POCI}(p,q) &= \mathrm{Re}(\psi) \\
&= \frac{\sin\frac{1}{2}\left(\frac{2\pi}{N}k+\frac{\pi}{N}\right)+\sin\left(\left(N-\frac{1}{2}\right)\left(\frac{2\pi}{N}k+\frac{\pi}{N}\right)\right)}{2\sin\frac{1}{2}\left(\frac{2\pi}{N}k+\frac{\pi}{N}\right)} \\
&= \frac{1}{2}+\frac{\sin\left(\left(N-\frac{1}{2}\right)\left(\frac{2\pi}{N}k+\frac{\pi}{N}\right)\right)}{2\sin\frac{1}{2}\left(\frac{2\pi}{N}k+\frac{\pi}{N}\right)}
\end{aligned}
\tag{A·8}
$$

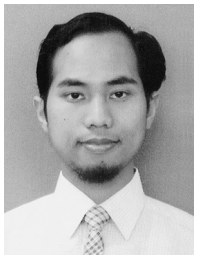

Khoirul Anwar graduated cum laude from the Dept. of Electrical Engineering, Bandung Institute of Technology (ITB), Indonesia, in 2000. After serving as an information technology specialist in a domestic company, he completed the M.S. program in Information Science at Nara Institute of Science and Technology, Japan, in 2005. Since then, he has been in the doctoral program. He has been engaged in research on mobile communications, OFDM in satellite communication, WiMAX, and PAPR reduction of OFDM and wavelet systems. He received Best Student Paper Award from IEEE Radio & Wireless Symposium 2006, California, USA.

Masato Saito received the B.S., M.S., and Ph.D. degrees from Nagoya University, Japan in 1996, 1998, 2001, respectively. He is currently an Assistant Professor of the Graduate School of Information Science at Nara Institute of Science and Technology (NAIST), Japan. From April 2007 he is a visiting researcher at ARC Special Research Centre for Ultra-Broadband Information Networks (CUBIN), the University of Melbourne, Australia. His current research interests include mobile communications, multi-hop networks, multicarrier modulation systems, CDMA systems, packet radio networks. Dr. Saito is a member of IEEE.

Takao Hara graduated from the Dept. of Communication Engineering, Osaka University, in 1968 and joined Fujitsu. In the Satellite Communication Research Department of Fujitsu Laboratories, he was engaged in research and development on digital satellite communication systems such as TDMA, SS/TDMA, and SCPC and burst modems. In 1980–1984, he was affiliated with Fujitsu USA. After returning to Japan, he has been engaged in research and development of TDMA systems and VSAT. In 2003, he completed the doctoral program at Nara Institute of Science and Technology, becoming a research associate in the same year. In 2006 he became a research staff member and in 2007 he became the associate professor. He has been engaged in research on mobile communications and satellite communication. He holds a Dr.Eng. degree.

Minoru Okada received the B.E. degree from the Dept. of Communications Engineering, University of Electro-Communications, in 1990, and the M.E. and Ph.D. degree both in Communications Engineering from Osaka University in 1992 and 1998, respectively. In 1993, he became a research associate at Osaka University. In 1999, he was a visiting scholar at Southampton University, U.K. In 2000, he became an associate professor of information science at Nara Institute of Technology, where he was appointed a professor in 2006. He has been engaged in research on mobile communications and digital broadcasting.